Journal of Hazardous Materials 203–204 (2012) 348–356

Contents lists available at SciVerse ScienceDirect

Journal of Hazardous Materials

journal homepage: www.elsevier.com/locate/jhazmat

# Investigation on the conditions mitigating membrane fouling caused by $TiO_2$ deposition in a membrane photocatalytic reactor (MPR) used for dye wastewater treatment

Rahul-Ashok Damodar [a], Sheng-Jie You [a,*], Guan-Wei Chiou [b]

[a] Department of Bioenvironmental Engineering and R&D Center for Membrane Technology, Chung Yuan Christian University, Chung li 320, Taiwan, ROC
[b] Department of Civil Engineering, Chung Yuan Christian University, Chung li 320, Taiwan, ROC

ARTICLE INFO

*Article history:*
Received 1 September 2011
Received in revised form
24 November 2011
Accepted 12 December 2011
Available online 19 December 2011

*Keywords:*
Membrane photoreactor
UV/$TiO_2$
Fouling mitigation
Zeta potential
AOP
Resistance

ABSTRACT

In this study, the effects of MPR's operating conditions such as permeate flux, solution pH, and membrane hydrophobicity on separation characteristics and membrane fouling caused by $TiO_2$ deposition were investigated. The extent of fouling was measured in terms of TMP and tank turbidity variation. The results showed that, at mildly acidic conditions (pH ~ 5), the turbidity within the tank decreased and the extent of turbidity drop increased with increasing flux for all the membranes. On the other hand, at pH ≥ 7, the turbidity remained constant at all flux and for all membranes tested. The fouling variation at different pH was closely linked with the surface charge (zeta potential) and hydrophilicity of both membrane and particles. It was observed that the charge differences between the particles and membranes accelerate the intensity of fouling and binding of $TiO_2$ particles on the membrane surface under different pH conditions. The presence of a very thin layer of $TiO_2$ can alter the hydrophilicity of the membranes and can slightly decrease the TMP (filtration resistance) of the fouled membranes. Besides, the resistance offered by the dense $TiO_2$ cake layer would dominate this hydrophilic effect of $TiO_2$ particles, and it may not alter the filtration resistance of the fouled membranes.



## 1. Introduction

Heterogeneous photocatalysis (UV/$TiO_2$ system) has been extensively researched and commercialized in the last two decades for its environmental applications. In this process, the pollutants are oxidized by the action of hydroxyl radical's generated by the photocatalyst (titanium dioxide, $TiO_2$) and ultraviolet (UV) photons. The hydroxyl radical is able to mineralize the majority of hazardous organic compounds to innocuous end-products [1–5]. The key advantage of this process is that photo-oxidation can be carried out under ambient conditions (atmospheric oxygen is used as the oxidant) and may lead to complete mineralization of organic carbon into $CO_2$ and $H_2O$. Moreover, the photocatalyst, $TiO_2$, is easily available, inexpensive, non-toxic and shows relatively high chemical stability [5–9].

The photoreactors described in the literature can be divided into two main groups, *viz.*, slurry photoreactor (in which $TiO_2$ suspended in the reaction mixture), and immobilized photoreactor (in which $TiO_2$ is fixed or supported on a carrier material). The slurry type photoreactor offers several advantages that include: high surface area for adsorption and reaction, high degradation rate, no mass transfer limitation, and simple reactor configuration. On the other hand, the photocatalyst immobilized on a support, within the photoreactor, usually shows lower degradation rates due to loss of photo-activity with operational time. However, application of suspended photocatalytic system is rather limited by the time consuming step of the photocatalyst separation from the treated water after detoxification. This process can be made ecologically and economically feasible by means of confining or recycling the photocatalyst within the treatment unit [10–13].

Recently, application of membrane separation technique has shown to solve the important issue of catalyst separation in a slurry type photocatalytic reactor [13]. The separation characteristic of membrane also allows maintaining, constantly, the desired levels of $TiO_2$ suspension within the photoreactor. Among the different MPR configurations available, catalyst in suspension confined by means of a submerged membrane configuration (a hollow fiber or flat sheet) appears to be more feasible for industrial/practical applications [14–16]. Recent studies have proved that low-pressure membranes can effectively be used for separation of $TiO_2$ in submerged MPR system owing to its inherent advantages, such as low fabrication, maintenance and operating costs [16–19]. In MPR, both photocatalytic degradation reactions and $TiO_2$ separation are achieved simultaneously. Thus, the different operating conditions

* Corresponding author. Tel.: +886 32654931; fax: +886 32654933.
*E-mail address:* sjyou@cycu.edu.tw (S.-J. You).

0304-3894/$ – see front matter © 2011 Elsevier B.V. All rights reserved.
doi:10.1016/j.jhazmat.2011.12.027

**Table 1**
Characteristics of the membrane used in this study.

| Item | PAN | PVDF | PTFE |
|---|---|---|---|
| Manufacturer | C.M.T. | C.M.T. | C.M.T. |
| Material | Polyacrylonitrile | Polyvinylidene fluoride | Polytetrafluoro-ethylene |
| Pore size (μm) | 0.035 | 0.38 | 0.22 |
| Contact angle (°) | 54.6 ± 1.6 | 78.3 ± 3.4 | 120 ± 3.5 |

of MPR will simultaneously affect the photocatalytic degradation efficiency, as well as the separation (filtration) efficiency of the membrane. It was also reported that the operation of MPR was severely affected by fouling, caused by the accumulation of $TiO_2$ particles on the membrane surface during continuous filtration [14,20–22]. An analysis of fouling resistance on the membrane filtration process showed that a cake layer formation on the membrane surface was the main mechanism responsible for fouling [23,24]. The effect of different operating conditions of MPR on degradation efficiency was extensively studied and reported by many researchers [3,4,13,19,25,26], however, so far its effect on separation efficiency and fouling of the membrane was not reported in detail.

The efficiency of the photocatalytic degradation process is affected by several operating parameters such as: pH of the solution to be degraded, initial concentration of the target compound, UV light (source, intensity and exposure/depth of penetration), temperature, reactor configuration, aeration (intensity, bubble size, dissolve oxygen, and mixing/circulation rate), catalyst characteristics (type, size, and surface area) and loading, among others [4,6,13,25,26]. The selection of proper polymeric membranes is an important challenge in the UV/$TiO_2$ photocatalytic-membrane process. Chin et al. [27] studied the stability of different membrane materials, and the results from their study showed that polytetrafluoroethylene (PTFE), polyvinylidene fluoride (PVDF) and polyacrylonitrile (PAN) membranes possess the greatest stability and resistivity in comparison to other membrane types studied. The $TiO_2$ powders are very small (average particle size of Degussa P25 is about 21 nm). However, in aqueous media, the $TiO_2$ particle forms an aggregate within the micron range. Therefore, microfiltration (MF) process range (0.1–5 μm) easily meets such a size requirement of the $TiO_2$ particle separation process [21,28]. For a suspension system, zeta potential is an important index which reflects the intensity of attractive/repulsive force among particles and the stability of dispersion. The point of zero potential charge (zpc) of Degussa P25 $TiO_2$ particles is around $pH_{zpc}$ 6.3. Hence, the $TiO_2$ surface is positively charged under acidic medium (pH < 6.3) and negatively charge under basic medium conditions (pH > 6.3). Thus, $TiO_2$ particles form agglomerates when dissolved in water and its size depends on several factors, such as the chemical composition of the particle surfaces, the composition of the surrounding solvent, the environmental pH value and ions in the suspension [29]. The $TiO_2$ particle size distribution, its charge and membrane's surface charge in the aqueous medium are affected simultaneously by the solution pH and this may also affect the interaction between particle and membrane surface.

According to Huisman et al. [30], both, the amount of fouling and the reversibility of fouling are dependent on the zeta-potential of the feed suspension particles and the membrane surface. From this point of view, the membrane surface can either have a positive or a negative effect on the filtering process [31]. Therefore, the membrane's surface properties (such as hydrophobicity, pore size and charge), its operating flux and $TiO_2$ properties (such as particle size distribution and surface charge) at different pH of solution will greatly affect the membrane fouling caused by $TiO_2$ deposition. In this study, the effects of MPR operating conditions such as permeate flux, solution pH and membrane type (hydrophobicity) on separation characteristics and membrane fouling caused by $TiO_2$ deposition were investigated.

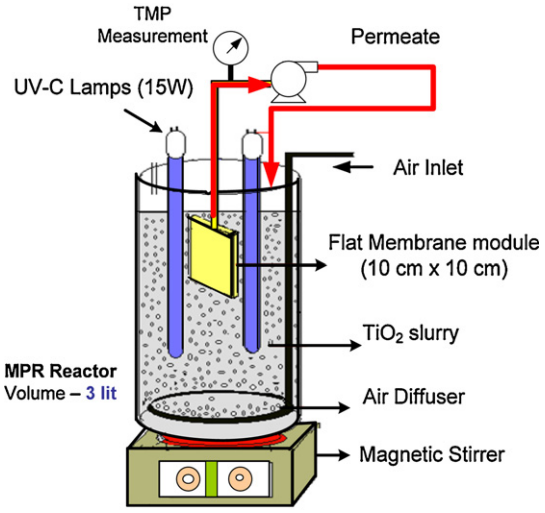


**Fig. 1.** Schematic of the membrane photocatalytic reactor (MPR) setup.

## 2. Materials and methods

### 2.1. Materials

Three kinds of flat sheet membranes such as PVDF, PAN and PTFE (provided by the R&D Center for Membrane Technology (CMT) of Chung Yuan Christian University, Taiwan) were tested in the MPR unit. PTFE and PVDF were relatively hydrophobic, while PAN was hydrophilic (Table 1). A highly dispersed and hydrophilic titanium dioxide powder (AEROXIDE® $TiO_2$ Degussa P 25) used in this experiment was supplied by Evonik *Degussa* Taiwan Ltd. The reactive black-5 (RB5, $C_{26}H_{21}N_5Na_4O_{19}S_6$; Mol Wt 991) dye was used as a model pollutant for this study.

### 2.2. Membrane photocatalytic reactor setup

The lab-scale MPR setup (Fig. 1) was fabricated using cylindrical glass (V 3 L) consisting of two UV-C lamps (15 W, 254 nm). One flat sheet membrane module (size 10 cm × 10 cm, with effective filtration area 0.01515 $m^2$) was placed at the middle and center of a tank, and surrounded by UV lamps. The solution was mixed using a magnetic stirrer. Aeration (flow rate 1.5 L/min) was provided through an air diffuser placed at the bottom of the tank in order to maintain the desired dissolved oxygen concentration and for mixing. Initially, few batch experiments were performed (in a same reactor without membranes), at different $TiO_2$ concentrations (0–1 g/L) and UV light exposures (continuous, semi-continuous) in order to envisage the optimum catalyst dose UV exposure required for the different experiments. RB5 removal (at pH 6.7, $C_{dye}$ 100 mg/L) was monitored by measuring the absorbance at 595 nm and true color (ADMI) removal was measured using a spectrophotometer, as per the standard procedure provided by Taiwan EPA Standard Methods.

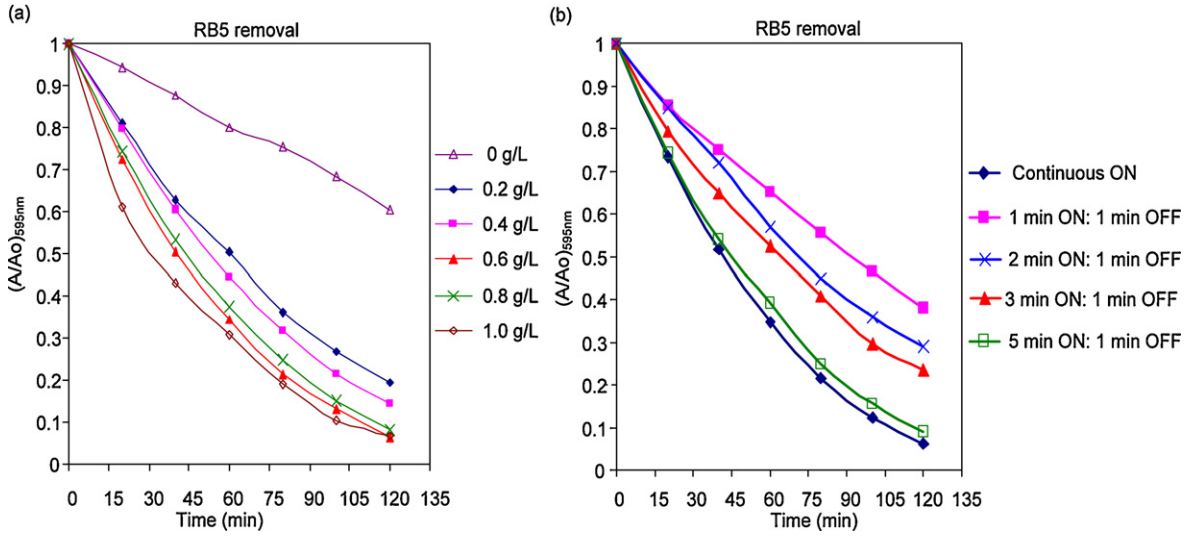


**Fig. 2.** (a) Effect of $TiO_2$ concentration on RB5 dye decolorization (UV exposure-continuous ON). (b) Effect of UV exposure on RB5 dye decolorization ($C_{TiO_2}$ 0.6 g/L, $C_{dye}$ 100 mg/L).

### 2.3. Experimental procedure

The experiments were carried out in batch recirculation mode. The permeate was withdrawn at a constant flux and recycled back to the tank. The concentration of Degussa P25 $TiO_2$ catalyst used in all the experiments (about 0.6 g/L) and UV light exposure (5 min ON and 1 min OFF cycle) was selected from batch trials, in which it found to be the optimum for reactive black-5 (RB5) dye degradation (dye concentration at 100 mg/L). The pH of $TiO_2$ slurry was adjusted by the addition of either HCl (1 M) or NaOH (1 M). The turbidity of tank solution and permeate were measured at a regular interval of time. The slurry $TiO_2$ concentration was estimated from turbidity *vs* concentration calibration curves. The permeate flux and TMP were also monitored regularly. The effects of pH (at 5, 7 and 9) and permeate flux (at 8, 12 and 16 mL/min, *i.e.*, 32, 48 and 64 L/m$^2$ h) on membrane fouling caused by $TiO_2$ deposition were investigated in a batch MPR using three different hydrophobic membranes, *viz.*, PVDF, PAN and PTFE, respectively. All the experiments were carried out for about 7 h and operated at a constant flux condition.

## 3. Results and discussion

### 3.1. Batch decolorization of RB5 dye

In heterogeneous photocatalysis, the catalyst concentration and UV exposure plays an important role in the chemical reactions and has a significant effect on the process degradation efficiency. Fig. 2(a) and (b) shows the effect of $TiO_2$ concentration and UV exposure on RB5 removal efficiency. It was observed that the rate of removal was high during the initial stages, as seen from steeper slopes, but at later stages the rate of removal decreased slightly. This may be due to the formation of intermediates, which may also be absorbing the photons from the UV light thereby competing with the dye molecule. It was observed that the degree of de-colorization of RB5 dye increased with increasing amount of $TiO_2$ photocatalyst, reaching the highest value at a catalyst loading of 0.6 g/L, and then remained almost constant above this concentration level. This behavior can be attributed to the shielding effects at higher catalyst concentrations, wherein the suspended $TiO_2$ reduces the

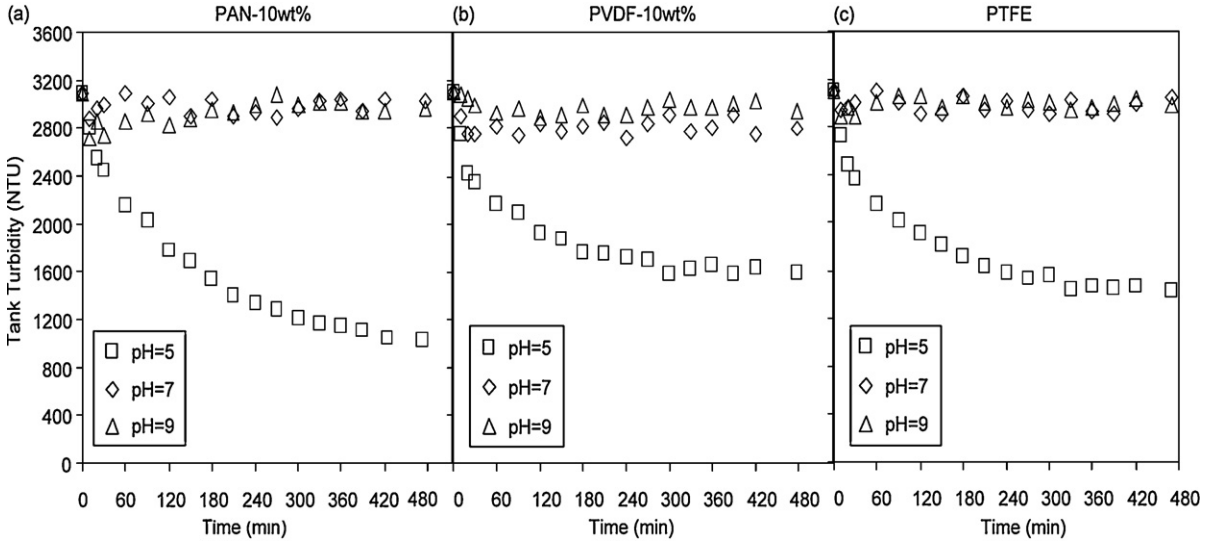


**Fig. 3.** Effect of pH on fouling of three different membranes (measured in terms of tank turbidity variation) (at flux 64 L/m$^2$ h, $C_{TiO_2}$ 0.6 g/L, and UV exposure – 5 min ON and 1 min OFF cycle).

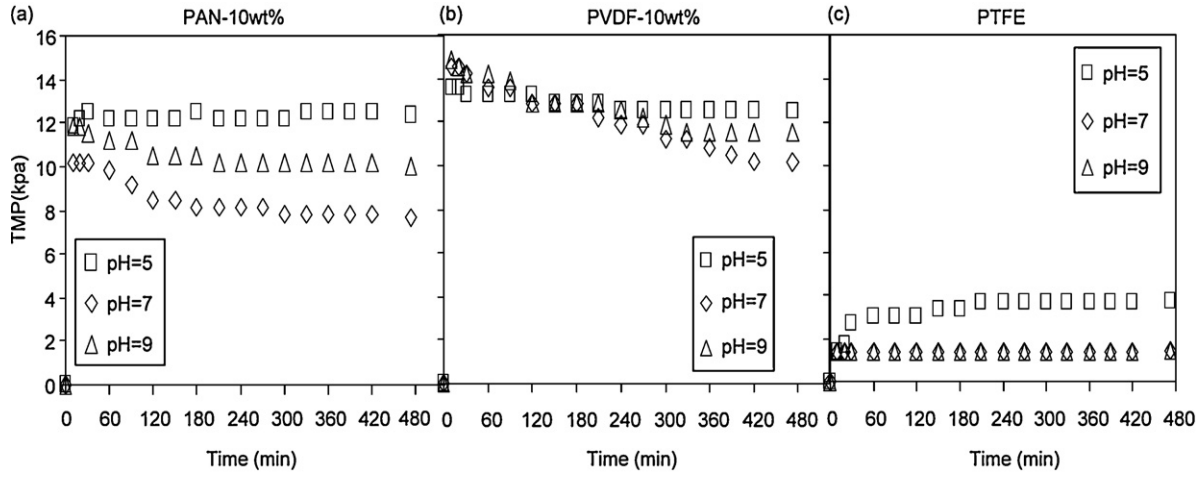


**Fig. 4.** Effect of pH on fouling of three different membranes (measured in terms of TMP variation) (at flux 64 L/m$^2$ h, $C_{TiO_2}$ 0.6 g/L, and UV exposure – 5 min ON and 1 min OFF cycle).

penetration of light into the solution. Since the active sites are proportional to the catalyst concentration, it will affect the color removal significantly [32]. When the catalyst loading is increased, there is an increase in the surface area of the catalyst available for adsorption and degradation. On the other hand, an increase of the photocatalyst concentration increases the solution opacity leading to a decrease in the penetration of the photon flux in the reactor [33]. As a result, the rate of dye degradation also increased with an increase in the mass of a catalyst present in the solution. However, above a certain loading, the dye degradation rate becomes independent of the catalyst amount, and thereafter remained constant with an increase in the catalyst concentration [13].

It was also observed that the exposure of UV light at a cycle condition of "5 min ON and 1 min OFF" performed similar to the continuous exposure condition. Therefore, these results revealed that semi-continuous UV exposure at a certain combination could also show similar dye degradation efficiencies, as observed during continuous UV exposure. This cyclic UV exposure mode requires a slightly lower fraction of total energy consumption when compared to the continuous UV exposure mode, and thus its use can lead to substantial cost saving without compromising the degradation rate. Hence, the concentration of $TiO_2$ catalyst 0.6 g/L and UV light exposure (5 min ON and 1 min OFF cycle) was selected as the optimum conditions for further studies.

### 3.2. Effect of pH on fouling

Figs. 3 and 4 show the effect of pH on fouling caused by $TiO_2$ deposition, which was measured in terms of tank turbidity and TMP variation, respectively, for three different hydrophobic membranes. Experiments were carried out at a constant flux condition and in batch recirculation mode. So, decrease in tank turbidity represents the loss of $TiO_2$ due to fouling caused by $TiO_2$ deposition during filtration. On the other hand, the TMP rise represents the resistance offered by the fouling $TiO_2$ cake layer accumulated during filtration. Results showed that at acidic pH ~ 5, the tank turbidity decreased with time and at pH ≥ 7, the tank turbidity dropped slightly and remained almost constant at a certain value throughout the experiment run. All the membranes showed similar trends. The decrease in turbidity at pH 5 indicated the fouling caused by $TiO_2$ deposition on the membrane surface. It was also visually observed that the $TiO_2$ fouling cake layer accumulated on the membranes surface was very dense at pH ~ 5 and very thin at pH ≥ 7. The permeate turbidity of all the membranes were below 4 NTU under all pH conditions tested (data not shown).

Depending on the membrane type, the TMP (filtration resistance) showed some interesting trends at different pH conditions. At pH = 5, the TMP value remained almost stable for PAN and PVDF membranes, while the TMP value increased for PTFE. However, at pH ≥ 7, the TMP value dropped slightly from its initial value for PAN and PVDF membrane and remained constant for the PTFE membrane. This behavior was closely linked with the surface charge (zeta potential) and hydrophilicity of both membrane and particles. $TiO_2$ particles are hydrophilic in nature and in the presence of UV light/water, its hydrophilicity increases due to production of OH groups under UV/water exposure. Thus, the deposition of $TiO_2$ particle's layer on the membrane surfaces during filtration might alter the hydrophilicity of membrane surface. At pH ≥ 7, the presence of very thin layer of $TiO_2$ might have altered the hydrophilicity of the membranes that resulted in a slight decrease in TMP (filtration resistance) for hydrophilic PAN and PVDF membranes. Whereas, at pH ~ 5, the resistance offered by dense $TiO_2$ cake layer might have dominated this hydrophilic effect of $TiO_2$ particles and resulted in no drop of TMP for hydrophilic PAN and PVDF membranes or rise of TMP for highly hydrophobic PTFE membrane. Thereby, the combined effect of $TiO_2$ cake thickness and hydrophilicity of membranes and $TiO_2$ particles can affect the TMP (filtration resistance) variation during the experiment.

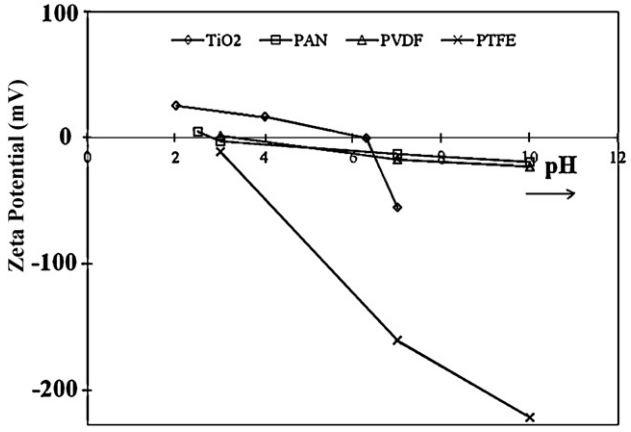


**Fig. 5.** The effect of pH on surface charge (Zeta potential, mV) of $TiO_2$ particles and all three membranes.

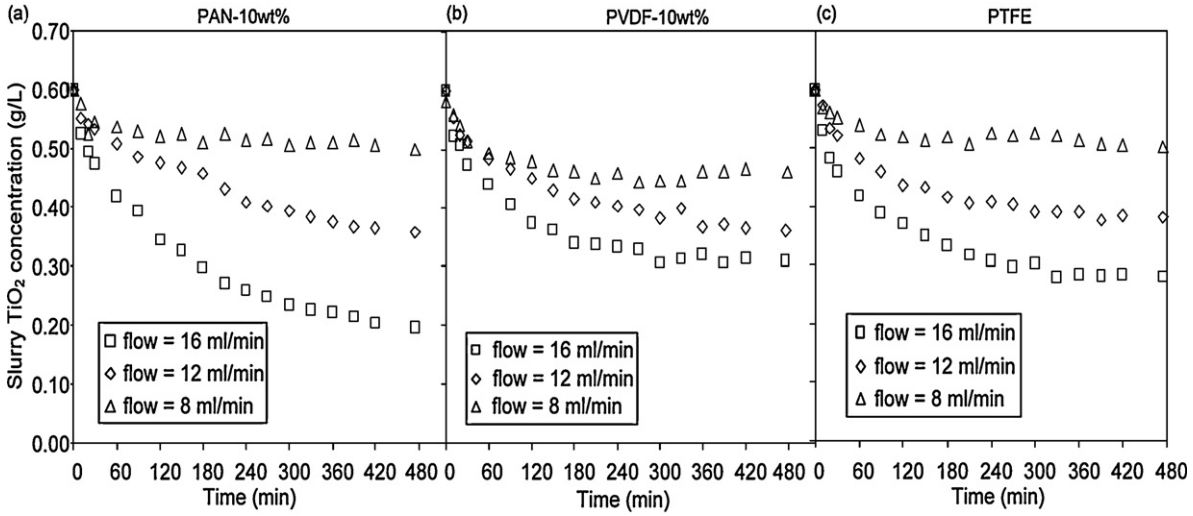


**Fig. 6.** Effect of flux on fouling of three different membranes (measured in terms of $TiO_2$ slurry concentration variation) (at pH 5, $C_{TiO_2}$ 0.6 g/L and UV exposure – 5 min ON and 1 min OFF cycle).

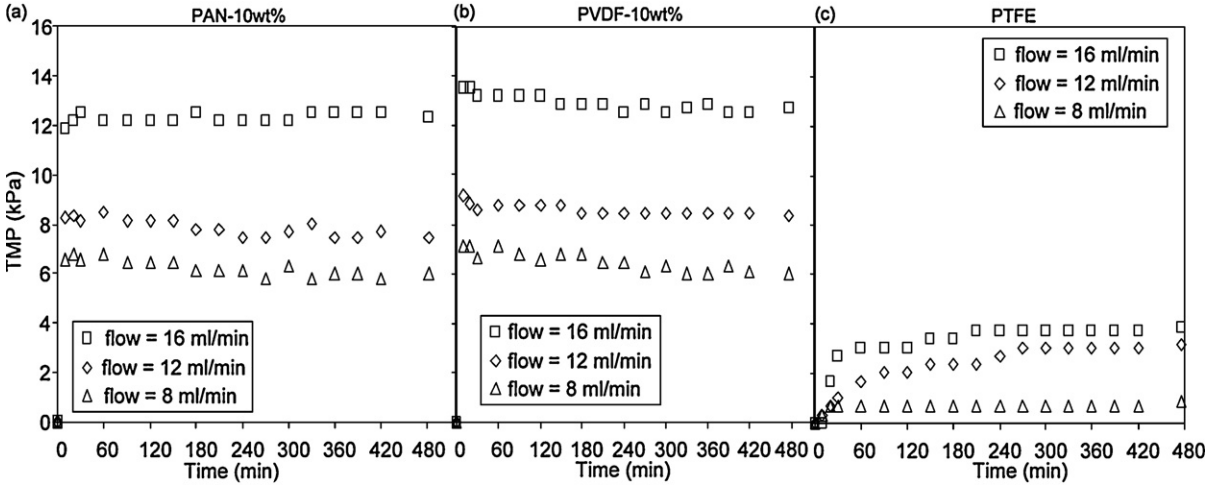


**Fig. 7.** Effect of flux on fouling of three different membranes (measured in terms of TMP variation) (at pH 5, $C_{TiO_2}$ 0.6 g/L and UV exposure – 5 min ON and 1 min OFF cycle).

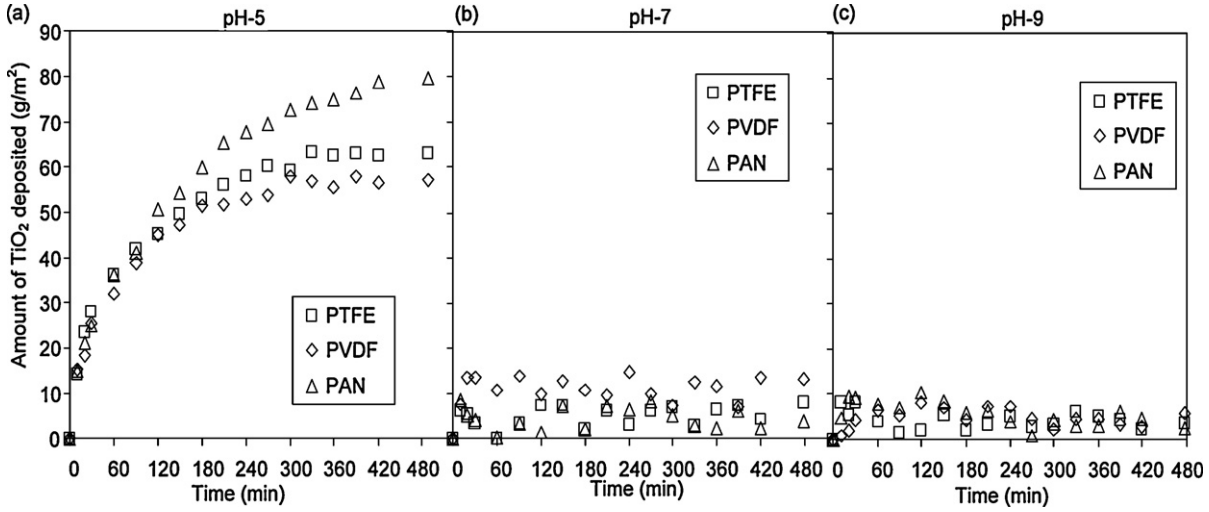


**Fig. 8.** The comparison of fouling of different membranes (measured in terms of amount of $TiO_2$ deposited) (at flux 64 L/$m^2$ h, $C_{TiO_2}$ 0.6 g/L and UV exposure – 5 min ON and 1 min OFF cycle).

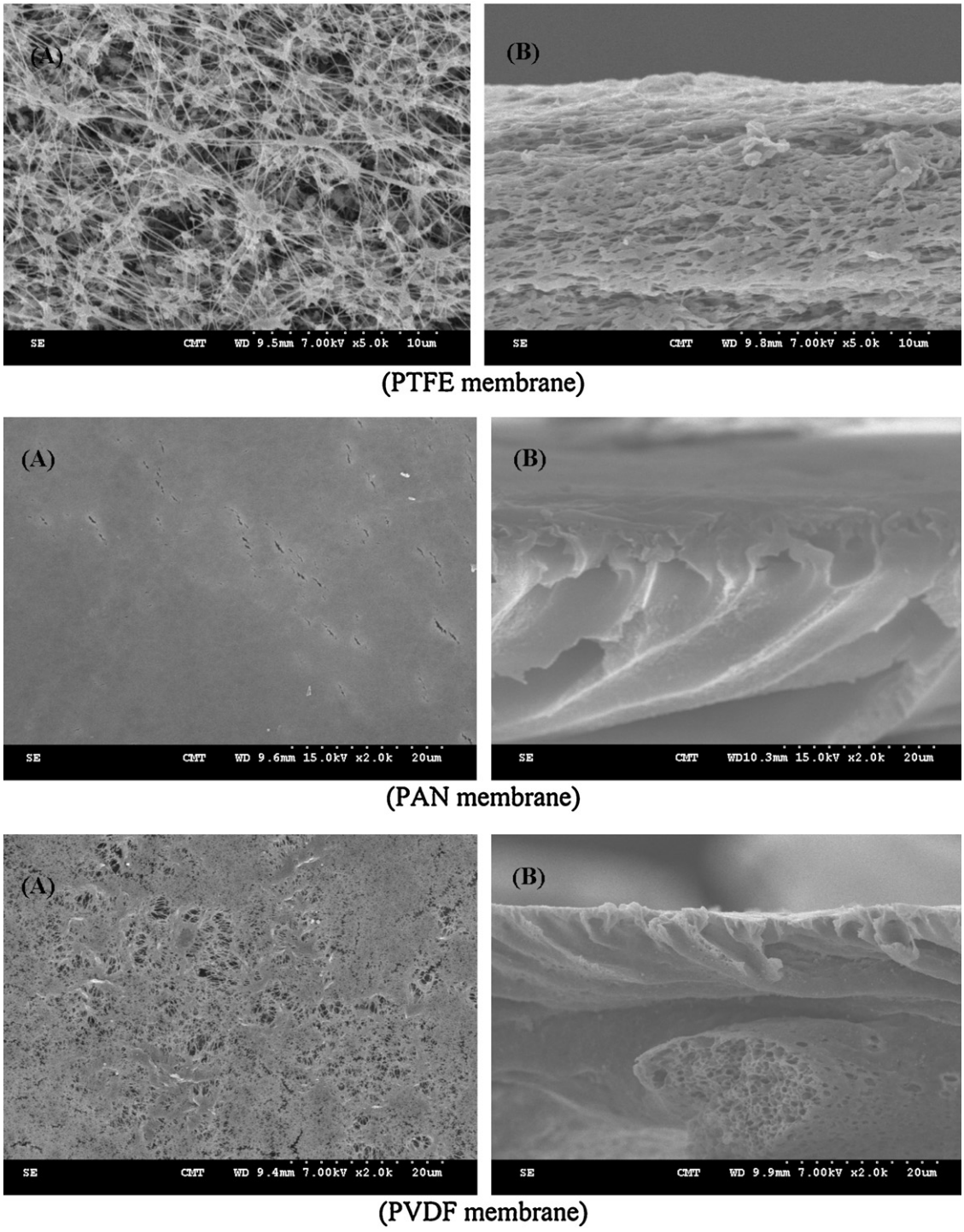


**Fig. 9.** The SEM images (a) top view and (b) cross section view of three different membranes.

pH is a complex parameter since it is related to ionization state of the surface, as well as that of reactant and products. It also influences the interaction between particles and membranes [34–36]. Fig. 5 shows the effect of pH on surface charge (Zeta potential, mV) of $TiO_2$ particles and all three membranes. The solution pH greatly influences the surface charges of the $TiO_2$ photocatalyst. For pH's higher than zero potential charge (ZPC) of titania, the surface becomes negatively charged and *vice versa* according to following two surfacial acid-basic equillibria [29,34,37] (Eqs. (1) and (2)):

$$\text{pH} > \text{ZPC} : \text{TiOH} + \text{OH}^- \rightarrow \text{TiO}^- + \text{H}_2\text{O} \quad (1)$$

$$\text{pH} < \text{ZPC} : \text{TiOH} + \text{H}^+ \rightarrow \text{TiOH}_2{}^+ \quad (2)$$

From Fig. 5, it is clearly evident that the $TiO_2$ is positively charged at pH < 6.3 and negatively charged at pH > 6.3. Whereas, PAN, PVDF and PTFE membranes were negatively charged at pH > 3. Therefore, this charge difference between particles and membranes might have also affected the fouling propensity under different pH conditions. At pH ≥ 7, the membranes and $TiO_2$ particles possessed the same charge (a negative), and this could be one of the reasons for low fouling at this pH conditions. Furthermore, at this condition, the $TiO_2$ also binds weakly on the membrane

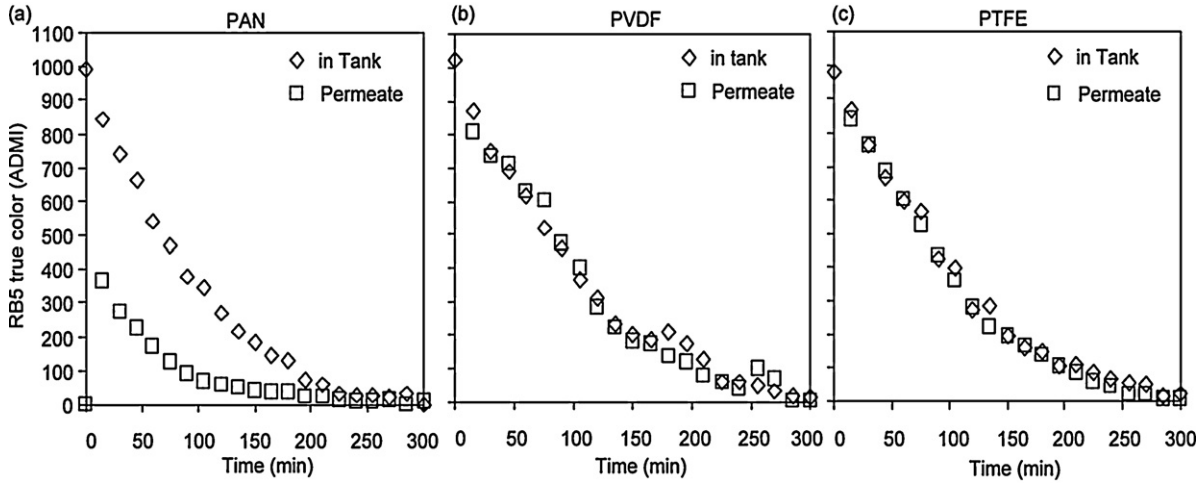


**Fig. 10.** The RB5 true color (ADMI) removal (within tank and permeate) using different membranes (at pH 7, flux 64 L/m$^2$ h, $C_{TiO_2}$ 0.6 g/L, $C_{dye}$ 100 mg/L and UV exposure – 5 min ON and 1 min OFF cycle).

surface and thus the resultant fouling layer might easily dislodge by surrounding turbulence. This phenomenon was clearly visible at this pH condition, as tank turbidity showed a slightly increasing and declining trend during the filtration run (Fig. 3). However, at pH = 5, the $TiO_2$ particles became positively charged, while all the membranes were negatively charged and due to this charge difference, at this pH condition, fouling rate accelerated. This charge difference can also result in the binding of $TiO_2$ particles on the membrane surface more strongly than that at other pH conditions. At this condition, it is advisable to supply a strong shear force (through aeration) in order to dislodge and to reduce fouling layer accumulation. The results from this study revealed that the determination of pH condition based on membrane fouling comparison will be more beneficial than those based on the pollutant degradation rate/efficiency. Or we need to choose the operating pH condition in such a way that it could minimize fouling as well as maximize degradation efficiency.

### 3.3. Effect of flux on fouling

All three membranes showed a similar tank turbidity variation trend under the tested flux conditions (at 8, 12 and 16 mL/min, *i.e.*, 32, 48 and 64 L/m$^2$ h), similar to those observed at different pH conditions (*i.e.*, severe fouling at pH ~ 5 and less fouling at pH ≥ 7). Figs. 6 and 7 show the effect of flux on fouling caused by $TiO_2$ deposition at pH ~ 5, which was measured in terms of $TiO_2$ slurry concentration and TMP variation, respectively, for the three hydrophobic membranes. The extent of $TiO_2$ slurry concentration drop (from 0.6 g/L to 0.2 g/L) indicates the fouling propensity. At pH ~ 5, as the flux increases, the $TiO_2$ slurry concentration drops rapidly for all the three membranes. On the other hand, as the flux increased from 32 to 64 L/m$^2$ h, more and more amount of $TiO_2$ particles accumulated on the membrane surface thus resulting in a substantial drop in slurry concentration. This reduction of slurry concentration due to fouling will also antagonistically affect the degradation efficiency of the MPR. At pH ≥ 7, an increase in the flux from 32 to 64 L/m$^2$ h did not show much difference in the fouling characteristics (data not shown).

The TMP variation at different flux levels showed a similar trend, as those envisioned at different pH conditions (*i.e.*, a slight decrease in TMP at pH ~ 5 and a nearly constant TMP at pH ≥ 7). At pH ~ 5 (Fig. 7), the TMP was almost constant throughout the experimental run for the hydrophilic PAN and PVDF membranes, respectively, while the TMP increased with operational time for the highly hydrophobic PTFE membrane at all flux conditions tested. The results also showed that the TMP increased linearly with an increase in the flux for all the membranes. The extent of TMP drop for PAN and PVDF membrane at pH ≥ 7 increased with increasing permeate flux (data not shown). These observations are similar to the observations made by Choo et al. [38]. Choo et al. [38] studied the effect of flux (15–100 L/m$^2$ h) on TMP variation using hollow fiber membranes at the following conditions: pH 7.0; humic acid concentration 10 mg/L (as TOC); $TiO_2$ dose 0.5 g/L; and UV irradiation 8 W. The authors observed a similar TMP trend at different flux conditions. As expected, the higher the flux, the larger the suction pressure. In addition, the suction pressure at each flux (15–70 L/m$^2$ h) applied was maintained at a nearly constant level during MPR operation (time 250 min), although a slight increase of pressure with time was observed at an extremely high flux of 100 L/m$^2$ h in the submerged photoreactor.

### 3.4. Extent of fouling of different membranes

Fig. 8 shows the comparison of fouling in terms of amount of $TiO_2$ deposited (g/m$^2$ of membrane filtration area) for different membranes at different pH conditions. Depending on membrane type, nearly 55–80 g/m$^2$, 5–15 g/m$^2$, and 4–9 g/m$^2$ of $TiO_2$ were deposited at pH 5, 7 and 9, respectively. At pH = 5, the amount of $TiO_2$ deposited increased with time for all the membranes. But all the membranes fouled to a similar extent, during 180 min of filtration and then the PAN membranes showed slightly higher fouling when compared to PVDF and PTFE membranes. Whereas at pH ≥ 7, the amount of $TiO_2$ deposited remained almost constant (slightly lower than the initial value) and the extent of fouling was similar for all the membranes. Fig. 9 shows the SEM images (a) top view (b) cross section view of three different membranes. The SEM images showed that the PAN membrane is much denser membrane in comparison to the PVDF and PTFE membrane. So this could be one reason PAN showed slightly higher fouling as compared to other two membranes.

### 3.5. RB5 color removal performance at low fouling and optimum conditions

The performance of RB5 true color (ADMI) removal was tested at the low fouling and optimum conditions of MPR (*i.e.*, pH 7, flux 64 L/m$^2$ h, $C_{TiO_2}$ 0.6 g/L, $C_{dye}$ 100 mg/L and UV exposure – 5 min ON and 1 min OFF cycle) using all the three membranes.

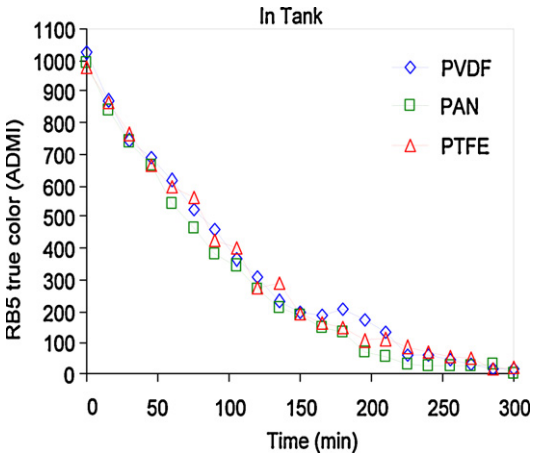


**Fig. 11.** The comparison of RB5 true color (ADMI) removal by different membranes (at pH 7, flux 64 L/m$^2$ h, $C_{TiO_2}$ 0.6 g/L, $C_{dye}$ 100 mg/L and UV exposure – 5 min ON and 1 min OFF cycle).

The MPR was operated in batch recirculation mode. The samples were collected at regular intervals of time from the tank bulk solution and permeate for comparing the color (ADMI) removal performance of three different membranes. Fig. 10 shows the RB5 color (ADMI) removal (within tank and permeate) using different membranes. The ADMI removal of permeate and a bulk solution (tank) in MPR operated using PAN membrane showed a different trend. Whereas, the ADMI removal of permeate and a bulk solution (tank) in MPR operated using PTFE and PVDF membranes showed similar trends. The PAN membranes was able to reject the color due to which the permeate ADMI showed slightly lower concentration as compared to bulk solution. Fig. 11 shows the comparison of RB5 color (ADMI) removal by different membranes within the bulk solution (tank). It was observed that the ADMI removal was almost similar for all the membrane due to similar operating conditions. This indicated that the lower ADMI in permeate of MPR operated using PAN membrane was solely due to rejection of ADMI by PAN membrane and this rejection did not affect the ADMI removal of bulk solution significantly. As mentioned earlier, it is clearly evident that the PAN membrane is denser (Fig. 9), while the PVDF and PTFE membranes had a porous structure. This could be the reason for observing slightly lower ADMI in permeate when compared to the bulk solution for PAN membrane.

## 4. Conclusions

Preliminary batch dye decolorization studies clearly demonstrated that the degree of de-colorization of RB5 dye increases with increasing amount of $TiO_2$ photocatalyst, reaching the highest value at catalyst loading at 0.6 g/L and then remained almost constant above this concentration. The exposure of UV light under the condition "5 min ON and 1 min OFF" performed similar to the continuous exposure condition. All three membranes showed a similar tank turbidity variation trend at all flux and pH conditions tested, *i.e.*, severe fouling at pH = 5 and low fouling at pH ≥ 7. The TMP and fouling variation at different pH were closely related to the surface charge (zeta potential) and hydrophilicity of both membrane and the particles. The charge differences between particle and membrane accelerated the intensity of fouling and binding of $TiO_2$ particles on the membrane surface at different pH conditions. The presence of a very thin layer of $TiO_2$ can alter the hydrophilicity of the membranes, and can also decrease the TMP (filtration resistance) of the slightly fouled membranes. Anew, the resistance offered by the dense $TiO_2$ cake layer could dominate the hydrophilic effect of $TiO_2$ particles but it may not alter the filtration resistance of the fouled membranes.

## Acknowledgements

This study was made possible by the financial support of the National Science Council, Taiwan (Project No. 99-2221-E-033-019-MY3).

## References

[1] A. Mills, S. Le Hunte, An overview of semiconductor photocatalysis, J. Photochem. Photobiol. A 108 (1997) 1–35.
[2] R.A. Damodar, S.J. You, H.H. Chou, Study the self cleaning, antibacterial and photocatalytic properties of $TiO_2$ entrapped PVDF membranes, J. Hazard. Mater. 172 (2009) 1321–1328.
[3] Y.-C. Lin, H.-S. Lee, Effects of $TiO_2$ coating dosage and operational parameters on a $TiO_2$/Ag photocatalysis system for decolorizing Procion red MX-5B, J. Hazard. Mater. 179 (2010) 462–470.
[4] S. Merabet, A. Bouzaza, D. Wolbert, Photocatalytic degradation of indole in a circulating upflow reactor by UV/$TiO_2$ process – influence of some operating parameters, J. Hazard. Mater. 166 (2009) 1244–1249.
[5] L. Reijnders, Hazard reduction for the application of titania nanoparticles in environmental technology, J. Hazard. Mater. 152 (2008) 440–445.
[6] V.A. Sakkas, M.A. Islam, C. Stalikas, T.A. Albanis, Photocatalytic degradation using design of experiments: a review and example of the Congo red degradation, J. Hazard. Mater. 175 (2010) 33–44.
[7] D. Suryaman, K. Hasegawa, S. Kagaya, T. Yoshimura, Continuous flow photocatalytic treatment integrated with separation of titanium dioxide on the removal of phenol in tap water, J. Hazard. Mater. 171 (2009) 318–322.
[8] K. Hashimoto, H. Irie, A. Fujishima, $TiO_2$ photocatalysis: a historical overview and future prospects, Jpn. J. Appl. Phys. 44 (2005) 8269–8285.
[9] G.L. Puma, A. Bono, D. Krishnaiah, J.G. Collin, Preparation of titanium dioxide photocatalyst loaded onto activated carbon support using chemical vapor deposition: a review paper, J. Hazard. Mater. 157 (2008) 209–219.
[10] A.K. Ray, A.A.C.M. Beenackers, Development of a new photocatalytic reactor for water purification, Catal. Today 40 (1998) 73–83.
[11] O.M. Alfano, D. Bahnemann, A.E. Cassano, R. Dillert, R. Goslich, Photocatalysis in water environments using artificial and solar light, Catal. Today 58 (2000) 199–230.
[12] L. Erdei, N. Arecrachakul, S. Vigneswaran, A combined photocatalytic slurry reactor-immersed membrane module system for advanced wastewater treatment, Sep. Purif. Technol. 62 (2008) 382–388.
[13] S. Mozia, Photocatalytic membrane reactors (PMRs) in water and wastewater treatment. A review, Sep. Purif. Technol. 73 (2010) 71–91.
[14] R. Molinari, L. Palmisano, E. Drioli, M. Schiavello, Studies on various reactor configurations for coupling photocatalysis and membrane processes in water purification, J. Membr. Sci. 206 (2002) 399–415.
[15] R.A. Damodar, S.J. You, Performance of an integrated membrane photocatalytic reactor for the removal of Reactive Black 5, Sep. Purif. Technol. 71 (2010) 44–49.
[16] S. Mozia, A.W. Morawski, M. Toyoda, M. Inagaki, Application of anatase-phase $TiO_2$ for decomposition of azo dye in a photocatalytic membrane reactor, Desalination 241 (2009) 97–105.
[17] D.P. Ho, S. Vigneswaran, H.H. Ngo, Photocatalysis-membrane hybrid system for organic removal from biologically treated sewage effluent, Sep. Purif. Technol. 68 (2009) 145–152.
[18] P. Le-Clech, E.-K. Lee, V. Chen, Hybrid photocatalysis/membrane treatment for surface waters containing low concentrations of natural organic matters, Water Res. 40 (2006) 323–330.
[19] V.C. Sarasidis, S.I. Patsios, A.J. Karabelas, A hybrid photocatalysis-ultrafiltration continuous process: the case of polysaccharide degradation, Sep. Purif. Technol. 80 (2011) 73–80.
[20] S.S. Chin, A.G. Fane, T.M. Lim, K. Chiang, Factors affecting the performance of a low-pressure submerged membrane photocatalytic reactor, Chem. Eng. J. 130 (2007) 53–63.
[21] H.B. Jiang, G.L. Zhang, T. Huang, J.Y. Chen, Q.D. Wang, Q. Meng, Photocatalytic membrane reactor for degradation of acid red B wastewater, Chem. Eng. J. 156 (2010) 571–577.
[22] R.A. Damodar, S.J. You, S.H. Ou, Coupling of membrane separation with photocatalytic slurry reactor for advanced dye wastewater treatment, Sep. Purif. Technol. 76 (2010) 64–71.
[23] Z.X. Zhong, W.X. Li, W.H. Xing, N.P. Xu, Crossflow filtration of nanosized catalysts suspension using ceramic membranes, Sep. Purif. Technol. 76 (2011) 223–230.
[24] H.K. Shon, S. Phuntsho, S. Vigneswaran, Effect of photocatalysis on the membrane hybrid system for wastewater treatment, Desalination 225 (2008) 235–248.
[25] U.G. Akpan, B.H. Hameed, Parameters affecting the photocatalytic degradation of dyes using $TiO_2$-based photocatalysts: a review, J. Hazard. Mater. 170 (2009) 520–529.
[26] X. Huang, Y. Meng, P. Liang, Y. Qian, Operational conditions of a membrane filtration reactor coupled with photocatalytic oxidation, Sep. Purif. Technol. 55 (2007) 165–172.

[27] S.S. Chin, K. Chiang, A.G. Fane, The stability of polymeric membranes in a $TiO_2$ photocatalysis process, J. Membr. Sci. 275 (2006) 202–211.
[28] W.M. Xi, S.U. Geissen, Separation of titanium dioxide from photocatalytically treated water by cross-flow microfiltration, Water Res. 35 (2001) 1256–1262.
[29] H. Lachheb, E. Puzenat, A. Houas, M. Ksibi, E. Elaloui, C. Guillard, J.M. Herrmann, Photocatalytic degradation of various types of dyes (Alizarin S, Crocein Orange G Methyl Red, Congo Red, Methylene Blue) in water by UV-irradiated titania, Appl. Catal. B 39 (2002) 75–90.
[30] I.H. Huisman, G. Trägårdh, C. Trägårdh, A. Pihlajamäki, Determining the zeta-potential of ceramic microfiltration membranes using the electroviscous effect, J. Membr. Sci. 147 (1998) 187–194.
[31] T. Moritz, S. Benfer, P. Arki, G. Tomandl, Influence of the surface charge on the permeate flux in the dead-end filtration with ceramic membranes, Sep. Purif. Technol. 25 (2001) 501–508.
[32] R.A. Damodar, K. Jagannathan, T. Swaminathan, Decolourization of reactive dyes by thin film immobilized surface photoreactor using solar irradiation, Sol. Energy 81 (2007) 1–7.
[33] S.P. Kamble, S.B. Sawant, V.G. Pangarkar, Batch and continuous photocatalytic degradation of benzenesulfonic acid using concentrated solar radiation, Ind. Eng. Chem. Res. 42 (2003) 6705–6713.
[34] A. Houas, H. Lachheb, M. Ksibi, E. Elaloui, C. Guillard, J.-M. Herrmann, Photocatalytic degradation pathway of methylene blue in water, Appl. Catal. B 31 (2001) 145–157.
[35] T. Sauer, G. Cesconeto Neto, H.J. José, R.F.P.M. Moreira, Kinetics of photocatalytic degradation of reactive dyes in a $TiO_2$ slurry reactor, J. Photochem. Photobiol. A 149 (2002) 147–154.
[36] R.A. Damodar, T. Swaminathan, Performance evaluation of a continuous flow immobilized rotating tube photocatalytic reactor (IRTPR) immobilized with $TiO_2$ catalyst for azo dye degradation, Chem. Eng. J. 144 (2008) 59–66.
[37] F. Zhang, J. Zhao, T. Shen, H. Hidaka, E. Pelizzetti, N. Serpone, $TiO_2$-assisted photodegradation of dye pollutants II. Adsorption and degradation kinetics of eosin in $TiO_2$ dispersions under visible light irradiation, Appl. Catal. B 15 (1998) 147–156.
[38] K.H. Choo, R. Tao, M.J. Kim, Use of a photocatalytic membrane reactor for the removal of natural organic matter in water: Effect of photoinduced desorption and ferrihydrite adsorption, J. Membr. Sci. 322 (2008) 368–374.